

DISPERSION OF TLM CONDENSED NODES IN MEDIA WITH ARBITRARY ELECTROMAGNETIC PROPERTIES

WE
1B

Vladica Trenkic, Christos Christopoulos and Trevor M. Benson

Department of Electrical and Electronic Engineering
University of Nottingham, Nottingham NG7 2RD, UK

Abstract – New analytical closed forms of the dispersion relation for TLM condensed nodes modelling general materials (stubbed symmetrical condensed node, symmetrical super-condensed node) are presented and validated by numerical results. The range of dispersion errors and bilateral behavior are fully explored and practical guidance is offered to users.

1 INTRODUCTION

This paper addresses the modelling of electromagnetic phenomena in materials with arbitrary ϵ_r, μ_r , using the TLM method with condensed nodes on a uniform mesh of node spacing d . This modelling may be achieved either by introducing open- and short-circuit stubs to the conventional symmetrical condensed node (SCN) [1], or by altering the characteristic impedances of the transmission-lines as established in the symmetrical super-condensed node (SSCN) [2].

It was shown in [2] that the SSCN requires less computer resources than the conventional stubbed SCN [1]. However, the dispersion characteristics must also be taken into account when selecting one of the two nodes for electromagnetic simulation. Dispersion in the stubbed SCN, based on numerical solutions of the general dispersion relation for TLM nodes [3], was investigated in [4], while here we obtain new closed-form analytical dispersion formulae and confirm their validity by results from our own simulations and from numerical solutions presented in [4]. We also validate the closed-form dispersion relation for the SSCN [5] and compare the dispersion characteristics of the two nodes (stubbed SCN and SSCN) in detail.

2 DISPERSION IN STUBBED SCN

The full dispersion analysis of the stubbed SCN (with six stubs) requires solution of an eigenvalue problem of 18th order [4] in terms of $\eta = \exp(jk_0d)$, where k_0 is the TLM mesh propagation constant. Taking

into account that two of the eigenvalues are constants representing non-propagating solutions ($\eta = 1$) [6] and that eigenvalues representing propagating solutions are found to be in reciprocal pairs (η, η^{-1}), the dispersion relation in general form can be written as an 8th-order polynomial in $\cos(k_0d)$.

An exact closed-form solution of a general 8th order polynomial does not exist, therefore eigenvalues cannot be expressed in closed-form. However, the above mentioned dispersion relation is a polynomial of second order in $\cos(k_xd), \cos(k_yd)$ or $\cos(k_zd)$, which allows its solution for a particular mode of propagation given by k_x, k_y, k_z , the cartesian components of the plane-wave propagation constant.

We have restricted our analysis here to cases when

Case 1: $\epsilon_r > 1, \mu_r = 1$ or $\mu_r > 1, \epsilon_r = 1$

Case 2: $\epsilon_r = \mu_r$

and for the following propagation directions:

- a) Propagation along a coordinate plane, e.g. $z = 0$.
- b) Propagation along a diagonal plane, e.g. $x = y$.

which contain most propagation modes of practical interest.

2.1 Case 1

The SCN for Case 1 is augmented by only three stubs (either open- or short-circuited), so that the size of matrices involved in the eigenvalue problem [4] is of 15th order. By eliminating solutions $\eta = \pm 1$ and grouping reciprocal eigenvalues, the dispersion relation can be expressed as a polynomial of 5th degree in $\cos(k_0d)$. A closed-form solution for $\cos(k_0d)$ cannot be found from the 5th order polynomial in general. However, the polynomial is of second order in $\cos(k_xd), \cos(k_yd)$ or $\cos(k_zd)$, which allows exact closed-form dispersion relations for particular modes of propagation.

The dispersion relation for Case 1 is presented here for subcases a, b in which the 5th degree polynomial splits into two parts, a quadratic and a cubic polynomial in $\cos(k_0d)$ and can be solved analytically. Two dispersion relations are obtained when $\epsilon_r \neq \mu_r$, corre-

sponding to different wave polarizations [4].

For Case 1a, assuming propagation in the $z = 0$ plane, the following SCN dispersion relations are obtained [4, 5]:

$$(\cos \theta - p \sin^2 \frac{x}{2})(\cos \theta - p \sin^2 \frac{y}{2}) - \cos^2 \frac{x}{2} \cos^2 \frac{y}{2} = 0 \quad (1)$$

$$\left[(\cos \theta - p \sin^2 \frac{x}{2})(\cos \theta - p \sin^2 \frac{y}{2}) - \cos^2 \frac{x}{2} \cos^2 \frac{y}{2} \right] \cdot \\ (\cos \theta + 1) - p \sin^2 \frac{x}{2} \sin^2 \frac{y}{2} [(p - 2) \cos \theta + p] = 0 \quad (2)$$

where $\theta = k_0 d$, $x = k_x d$, $y = k_y d$, $z = k_z d$.

When $\epsilon_r > 1$ and $\mu_r = 1$, $p = 1 - 1/\epsilon_r$ and equations (1) and (2) represent solutions for $H_z E_x E_y$ and $E_z H_x H_y$ propagation modes, respectively. Dual equivalents of equations (1) and (2) for the case $\epsilon_r = 1$, $\mu_r > 1$ hold with $p = 1 - 1/\mu_r$.

For Case 1b, with $k_x = k_y$, the dispersion relations obtained are:

$$\cos 2\theta + a_1 \cos \theta + a_2 = 0 \quad (3)$$

$$\cos 3\theta + b_1 \cos 2\theta + b_2 \cos \theta + b_3 = 0 \quad (4)$$

where coefficients a_1, a_2, b_1, b_2, b_3 are given by:

$$\begin{aligned} a_1 &= p(\cos x + \cos z - 2) \\ a_2 &= \frac{1}{2}(p - 1)(\cos^2 x + 2 \cos x \cos z - 1) - a_1 - p \\ b_1 &= p(3 \cos x + \cos z - 4) + 2 \\ b_2 &= (2p - 1)(p + 1) \cos^2 x + 2(p^2 + p - 1) \cos x \cos z \\ &\quad - 2p^2(3 \cos x + \cos z) + 4p^2 - 3p + 2 \\ b_3 &= [3p(p - 1) \cos z - 3p^2 + 2p - 1] \cos^2 x + p^2(\cos z - 1) \\ &\quad - [2(2p^2 - 2p + 1) \cos z - p(4p - 1)] \cos x - 2p + 1 \end{aligned}$$

Figures 1a,b show the dispersion in the stubbed SCN for Cases 1a,b respectively. Directions [100], [010] and [001] are given in Figure 1a for $\alpha = 90^\circ$, $\alpha = 0^\circ$ and in Figure 1b for $\beta = 0^\circ$, respectively. Direction [110] is given in Figure 1a for $\alpha = 45^\circ$ and in Figure 1b for $\beta = 90^\circ$, direction [111] is given in Figure 1b for $\beta = 45^\circ$, direction [120] is given in Figure 1a for $\alpha = \arctan(1/2) \approx 26.5^\circ$, direction [112] is given in Figure 1b for $\beta = \arctan(1/2) \approx 26.5^\circ$ etc.

The upper and lower sets of curves in Figure 1a correspond to equations (1) and (2), respectively. The upper and lower sets of curves in Figure 1b (as seen in the right-hand half of the plot) correspond to equations (3) and (4). In all cases the propagation error is calculated for $d/\lambda = 0.1$, where λ is the wavelength. The medium propagation constant is given by $k_m = 2k_0\sqrt{\epsilon_r\mu_r}$, while $|k| = (k_x^2 + k_y^2 + k_z^2)^{1/2}$.

Both parts of Figure 1 show the bilateral nature of the dispersion mentioned in [4], i.e. the coexistence of

positive and negative propagation errors. They show that dispersion curves at a given frequency converge as $\epsilon_r \rightarrow \infty$ or $\mu_r \rightarrow \infty$ and that the maximum positive propagation error occurs for the direction [110], i.e. for the propagation on the diagonal in a coordinate plane, whereas the maximum negative error occurs for axial propagation. Two sets of curves representing the orthogonal solutions (1) and (2) converge for axial propagation (Figure 1a). Similarly, solutions (3) and (4) converge for both axial propagation and propagation along the main space diagonal (Figure 1b). Note from Figures 1a,b that the relative propagation error corresponding to solutions (1) and (4) for the propagating directions [120], [210] and [112], [111], respectively, is practically independent of the material properties ϵ_r, μ_r .

2.2 Case 2

The 8th-order polynomial in $\cos(k_0 d)$, representing the general dispersion relation for the stubbed SCN, splits in Case 2 ($\epsilon_r = \mu_r$) into two identical parts which are themselves 4-th order polynomials in $\cos(k_0 d)$, and linear in $\cos(k_x d)$, $\cos(k_y d)$ or $\cos(k_z d)$. This means that for Case 2 there exists only one dispersion curve which confirms numerical results in [4].

The dispersion relation in Case 2 is:

$$\cos 4\theta + a_1 \cos 3\theta + a_2 \cos 2\theta + a_3 \cos \theta + a_4 = 0 \quad (5)$$

where coefficients $a_1 \dots a_4$ are given by:

$$\begin{aligned} a_1 &= 2p(S_1 - 3) + 4 \\ a_2 &= 4p(1 - 2p)S_1 + (3p - 1)(p + 1)S_2 + 15p^2 - 18p + 7 \\ a_3 &= 2p^2(5p - 2)S_1 - 2(3p^3 + 4p^2 - 5p + 2)S_2 \\ &\quad + 2p(p^2 + 6p - 3)S_3 - 2(7p^3 - 12p^2 + 12p - 4) \\ a_4 &= -2p(3p^2 - 2p + 1)S_1 + (2p^2 - p + 1)(5p - 3)S_2 \\ &\quad - 2p(7p^2 - 6p + 3)S_3 + 2p^3 + 9p^2 - 12p + 4 \end{aligned}$$

with

$$p = 1 - 1/\epsilon_r = 1 - 1/\mu_r$$

$$S_1 = \cos x + \cos y + \cos z$$

$$S_2 = \cos x \cos y + \cos y \cos z + \cos z \cos x$$

$$S_3 = \cos x \cos y \cos z$$

Figures 2a,b show the dispersion in the stubbed SCN for Cases 2a,b, respectively. They show that the propagation error is significantly bigger than for Cases 1a,b, and that the highest dispersion occurs for axial propagation. The dispersion curves at a given frequency converge when $\epsilon_r \mu_r \rightarrow \infty$ but at a slower rate than in Case 1. The propagation error is bilateral for smaller $\epsilon_r \mu_r$ and negative for larger $\epsilon_r \mu_r$.

3 DISPERSION IN SSCN

A general dispersion relation for the SSCN for all propagation modes has been obtained as [5]:

$$4\epsilon_r\mu_r \sin^2 \theta = 3 - \cos x \cos y - \cos y \cos z - \cos z \cos x \quad (6)$$

Figures 3a,b show the dispersion characteristics for the SSCN. They show that the propagation error is always positive (i.e. unilateral), it converges when $\epsilon_r\mu_r \rightarrow \infty$, it is independent of the ratio ϵ_r/μ_r for $\epsilon_r\mu_r = \text{const}$ and of the mode of propagation. The highest dispersion occurs on the main space diagonal. The dispersion curves for different $\epsilon_r\mu_r$ are practically equidistant which means that the range of dispersion error for given $\epsilon_r\mu_r$, as defined in [4], is constant.

4 VALIDATION

The analytical expressions presented here have been validated by numerical results from [4] and with our simulated results of the eigenvalue analysis of cubic resonators, using the simulation procedure similar to that of [4]. Note that in [4] the relative frequency error was calculated while here we calculate relative propagation error which has the opposite sign.

Numerical results are marked with diamond symbols and plotted in Figures 1-3a for the directions [010], [120], [110], [210], [100] and in Figures 1-3b for the directions [001], [112], [111], [110]. They are found to be in good agreement with the analytical plots, especially for propagation errors smaller than 1%.

Spurious propagating solutions detected in the SCN for the propagation on the main space diagonal [3, 6], are inherited in the stubbed SCN and the SSCN schemes and can be derived from equations (3)-(6). However they do not show significant impact on the results obtained from the simulations.

5 DISCUSSION AND CONCLUSIONS

Comparisons of the dispersion range of the stubbed SCN and the SSCN for different cases, can be done using the plots of Figures 1-3. For Case 1, the total range of the propagation error, assuming all propagation angles and solutions for $1 \leq \epsilon_r\mu_r < \infty$, is higher in the SSCN than in the stubbed SCN. However, the unique and unilateral dispersion characteristics observed for the SSCN and its constant dispersion range are potentially easier to correct, in contrast to the existence of two solutions and the bilateral dispersion detected in the stubbed SCN. For Case 2, the total range of dispersion in the SSCN is smaller compared to the SCN.

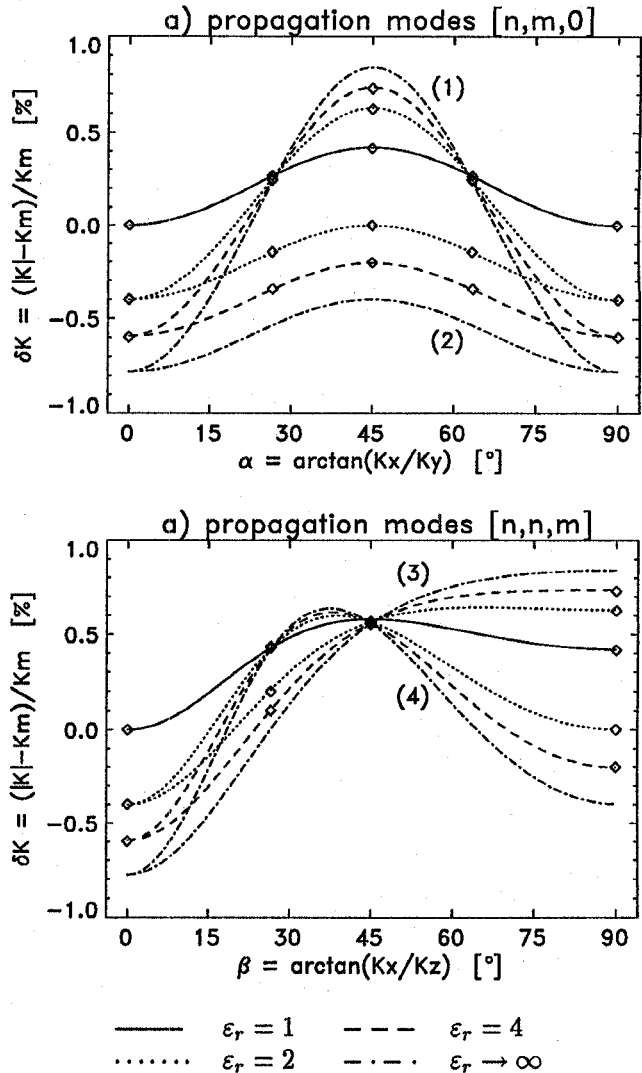


Figure 1: Stubbed SCN: Relative propagation errors for different ϵ_r , ($\mu_r = 1$)

- a) in the coordinate plane given by $z = 0$
- b) in the diagonal plane given by $x = y$

The choice of the TLM condensed node scheme for an actual simulation depends on the practical requirements. For example, when modelling dielectric materials (Case 1, $\mu_r = 1$), the three extra memory locations required in the stubbed SCN and the more time-consuming scattering procedure are justified by achieving more accurate results. In general cases ($\epsilon_r, \mu_r > 1$) when the SCN contains six stubs, it requires 50% more storage and approx. 20% more CPU time than the SSCN and, with dispersion characteristics similar to ones in Case 2, is less accurate for high ϵ_r, μ_r . In this case the SSCN is more efficient.

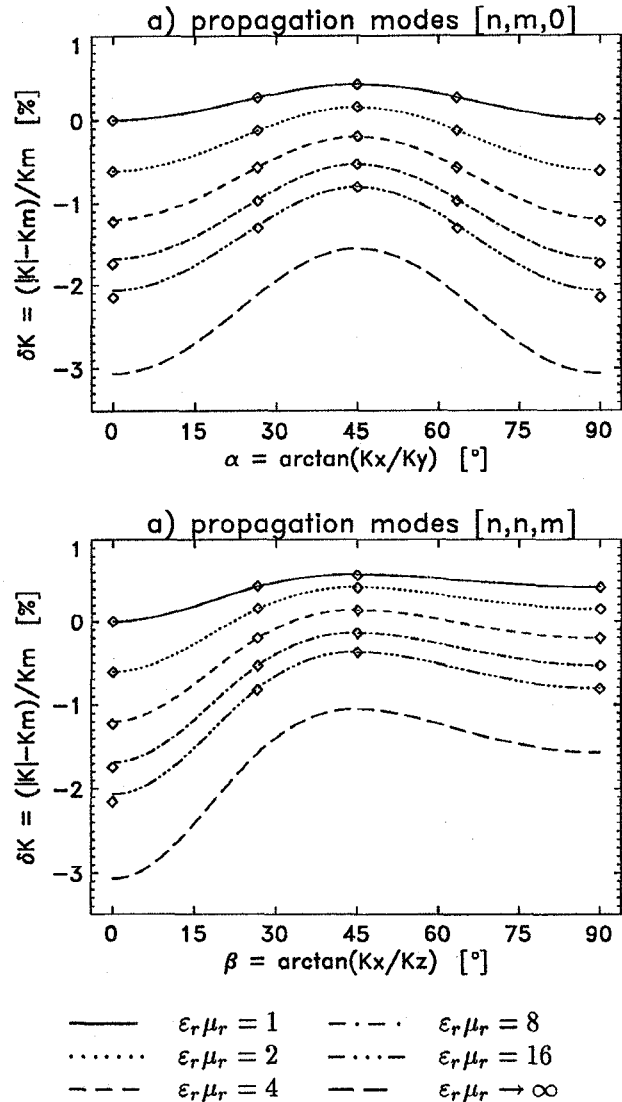


Figure 2: Stubbed SCN: Relative propagation errors for different $\epsilon_r \mu_r$ ($\epsilon_r = \mu_r$)

- a) in the coordinate plane given by $z = 0$
- b) in the diagonal plane given by $x = y$

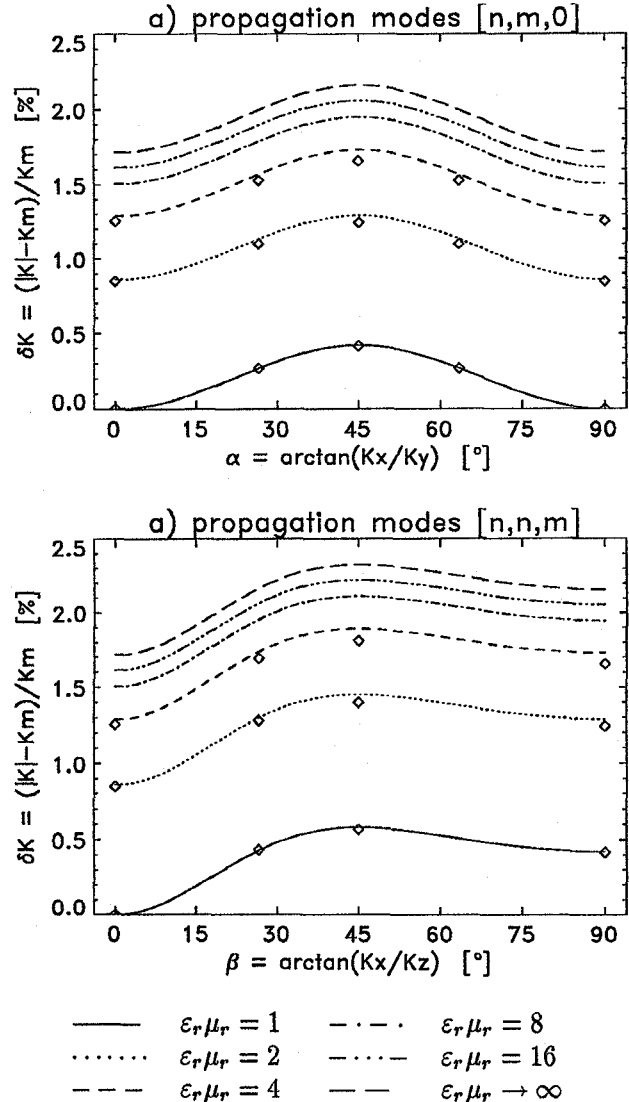


Figure 3: SSCN: Relative propagation errors for different $\epsilon_r \mu_r$

- a) in the coordinate plane given by $z = 0$
- b) in the diagonal plane given by $x = y$

REFERENCES

- [1] P. B. Johns. A symmetrical condensed node for the TLM method. *IEEE Trans., MTT-35(4)*:370–377, April 1987.
- [2] V. Trenkic, C. Christopoulos, and T. M. Benson. New symmetrical super-condensed node for the TLM method. *Electronics Letters*, 30(4):329–330, February 1994.
- [3] J. S. Nielsen and W. J. R. Hoefer. Generalized dispersion analysis and spurious modes of 2-D and 3-D TLM formulations. *IEEE Trans. Microwave Theory Tech.*, 41(8):1375–1384, 1993.
- [4] M. Celuch-Marcysiak and W. K. Gwarek. On the effect of bilateral dispersion in inhomogeneous symmetrical condensed node modelling. *IEEE Trans. Microwave Theory Tech.*, 42(6):1069–1073, 1994.
- [5] V. Trenkic, C. Christopoulos, and T. M. Benson. Dispersion analysis of TLM symmetrical super-condensed node. *Electronics Letters*, 30(25):2151–2153, December 1994.
- [6] M. Krumpelholz and P. Russer. On the dispersion in TLM and FDTD. *IEEE Trans. Microwave Theory Tech.*, 42(7):1275–1279, 1994.